Fatigue Crack Propagation in Short-Fiber Reinforced Plastics

Keisuke TANAKA[1], Takuya. KITANO[2], and Noboru EGAMI[1]

[1] Department of Mechanical Engineering, Meijo University, Shiogamaguchi, Tempaku-ku, Nagoya 464-8502, Japan, Fax: +81-(0) 832-1235, E-mail: ktanaka@meijo-u.ac.jp
[2] Graduate Student, Graduate School of Science and Technology, Meijo University

ABSTRACT. *The influence of fiber orientation on the crack propagation behavior was studied with single edge-notched specimens which were cut from an injection-molded plate of short-fiber reinforced plastics (SFRP), at five fiber angles relative to the loading axis, i.e. θ = 0° (MD), 22.5°, 45°, 67.5°, 90° (TD). Macroscopic crack propagation path was nearly perpendicular to the loading axis for the cases of MD and TD. For the other fiber angles, the crack path was inclined because the crack tended to propagate along inclined fibers. In the relation between crack propagation rate and the stress intensity factor range, ΔK, the propagation rate of fatigue cracks was slowest for MD, and increased with increasing fiber angle. When the crack propagation rate was correlated to $\Delta K/E$ (Young's modulus), the relations for different orientations merged together. The crack propagation rate was mainly controlled by ΔK at low rates and by the maximum stress intensity factor K_{max} at high rates. The existence of the core layer had an influence on the fatigue crack propagation behavior of injection-molded plates. It accelerated crack propagation in MD direction, and decelerated in TD direction.*

INTRODUCTION

SFRP are expected to be used more widely in order to reduce the weight of vehicles such as automobiles, because the injection molding process makes high-rate and economical production possible. Their application in fatigue-sensitive components has steadily increased in automobile industries. Under cyclic loading, fatigue cracks are formed relatively early in machine components and the propagation process occupies the most part of the fatigue life. The propagation behavior of fatigue cracks is anisotropic [1-4]. The path of crack propagation is influenced by the fiber orientation even if the applied load is uniaxial, and cracks often propagate under mixed mode condition.

In the present paper, the crack propagation behavior was studied with SFRP plates made by injection molding under the load ratio of 0.1 and 0.5. The influences of fiber orientation on the crack path and the crack propagation rate was studied from a viewpoint of fracture mechanics.

EXPERIMENTAL PROCEDURE

Specimens

The materials is a short-fiber reinforced brittle thermoplastics. The amount of fiber content was 20 wt%. Fatigue specimens were cut from an injection-molded plate with the in-plane dimensions of 80×80 mm and the thickness of 1 mm. Figure 1 shows the shape of test specimens which has a single edge notch of length 2 mm. The angle between molding and longitudinal directions was set to be five values: θ = 0° (MD), 22.5°, 45°, 67.5°, 90° (TD). Since the fiber direction of the skin layer of injection-molded plate is nearly along the molding flow direction, the angle θ means the angle between the fiber direction and the loading axis. In the following, the angle θ is called the fiber angle.

Injection-molded plates have a three-layer structure where two skin layers sandwich the core layer [5]. The thickness of the core layer of the present plates was about 0.15 mm. The core layer may influence the crack propagation behavior in the skin layer. To evaluate the influence of the core layer, specimens made of only skin layer were manufactured by thinning the 1mm thickness to 0.4 mm from the one side of the plate only for cases of MD, TD, and 45°. In this paper, the 1mm injection-molded plate is called IMP, and skin-layer plates SLP. Specimens made of only the matrix resin were also made from the injection-molded plate with thickness 1mm.

Fatigue Crack Propagation Tests

Fatigue tests were performed with a tension-compression electro-servo-hydraulic testing machine. Fatigue testing was done in air at room temperature under load-controlled conditions with the load ratio *R* of 0.1 and 0.5. The waveform of the cyclic load was triangular and the frequency was between 2.5 and 8 Hz.

The crack length was measured with a video microscope at the magnification of 100. The measured length of cracks was the projection of the crack on the plane perpendicular to the loading axis, and the sum of the crack length and the notch length was expressed as the total crack length *a* in this paper. The stress intensity factor was calculated by FEM by assuming the material as isotropic.

EXPERIMENTAL RESULTS AND DISCUSSION

Fatigue Crack Propagation Path

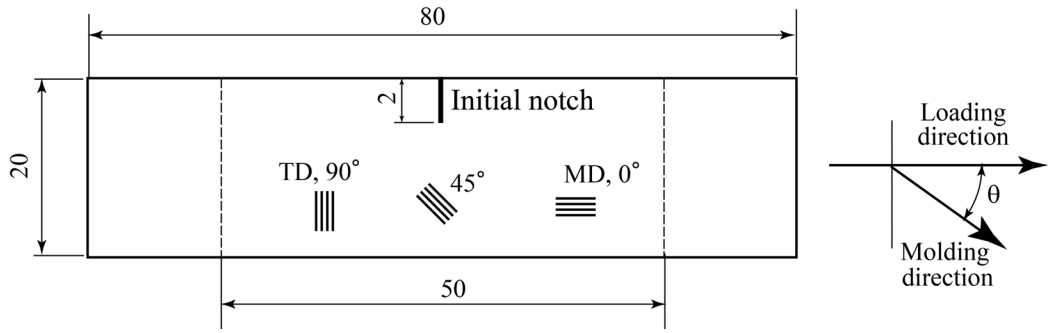

Figure 1. Shape and dimensions of specimen (in mm).

Optical micrographs of cracks for MD, 45°, and TD specimens of IMP fatigued under R = 0.1 are shown in Fig. 2, respectively, where the square region shown in (a), (c),(e) are enlarged in (b), (d), (f). For MD and TD specimens, the crack path is microscopically zigzag shaped and macroscopically straight perpendicular to the loading direction. On the other hands, the crack path of 45° specimen is inclined, making the angle of φ = 24.4° with respect to the plane perpendicular to the loading axis. The microscopic crack path is either in the matrix or along fibers. For MD specimens, the crack propagation is blocked by fibers and circumvents fibers along fiber surfaces, showing zigzag path. For TD specimens, the crack path is less tortuous following the fiber direction. For 45°

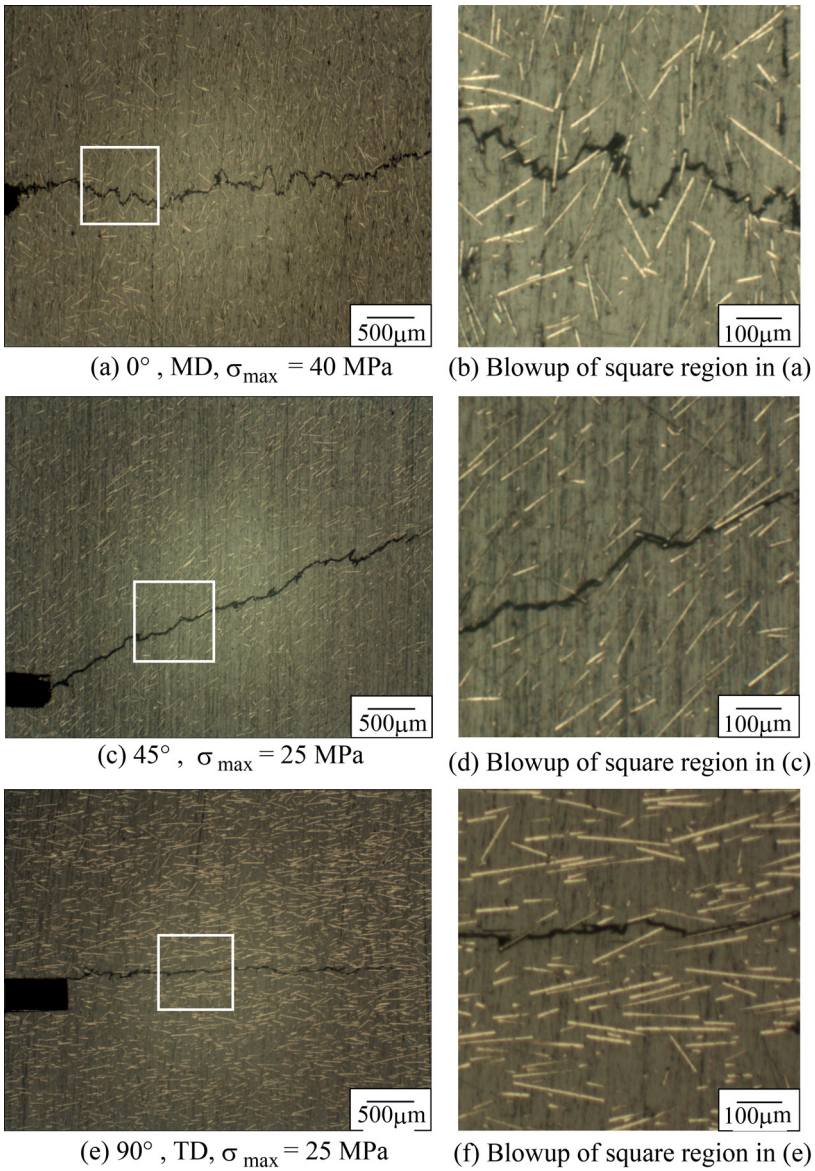

(a) 0° , MD, σ_{max} = 40 MPa (b) Blowup of square region in (a)

(c) 45° , σ_{max} = 25 MPa (d) Blowup of square region in (c)

(e) 90° , TD, σ_{max} = 25 MPa (f) Blowup of square region in (e)

Figure 2. Fatigue cracks of MD, 45°, TD specimens of IMP under R = 0.1.

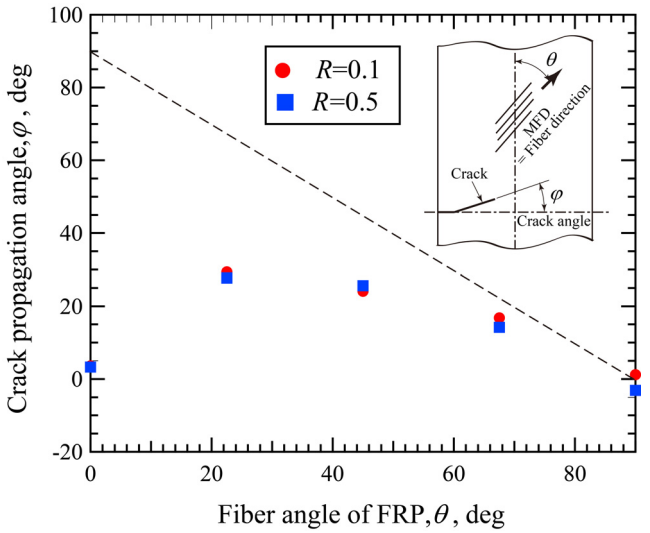

Figure 3. Relation between crack propagation angle and fiber angle.

specimens, the crack propagates nearly 45° along the fiber and turns to horizontal in the matrix. The macroscopic direction a combination of these two paths and is less than the fiber angle of 45°.

The macroscopic crack path for 22.5° and 67.5° specimens was not perpendicular to the loading axis. Figure 3 shows the change of crack propagation angle φ with the fiber angle θ for R = 0.1 and 0.5. The dotted line in the figure indicates the crack path is coincident to the fiber angle, i.e. $\varphi = 90 - \theta$ (deg). There is no big difference between R = 0.1 and 0.5. The crack angle increases with decreasing fiber angle, and takes a maximum at 22.5°. The crack angle for the cases of $\theta = 22.5°$, 45°, 67.5° is below the dotted line, because the macroscopic crack path consists of the matrix path with $\varphi \approx 0$ and fiber path with $\varphi \approx 90 - \theta$.

The macroscopic crack path of MD, TD specimens made of SLP was nearly perpendicular to the loading axis. The degree of crack tortuousness is slightly larger for SLP than for IMP. The inclined angle φ of 45° specimen of SLP was 28.5° which is larger than 24.4° for those of IMP.

Fatigue Crack Propagation Rate

Except MD and TD specimens, the macroscopic crack path is not perpendicular to the loading axis, so the crack is subjected to mixed loading of mode I and II. Here, for simplicity, the crack length is measured as the length projected to the plane perpendicular to the loading axis. Moreover, by neglecting material anisotropy, the stress intensity factor calculated based isotropic elasticity is employed as a fracture mechanics parameter.

Figure 4 shows the relation between the crack propagation rate, da/dN, and the range of stress intensity factor, ΔK, for IMP specimens with five different orientations and for the matrix resin. The data can be grouped into three: (1) MD and 67.5°, (2) 45°, 22.5°,

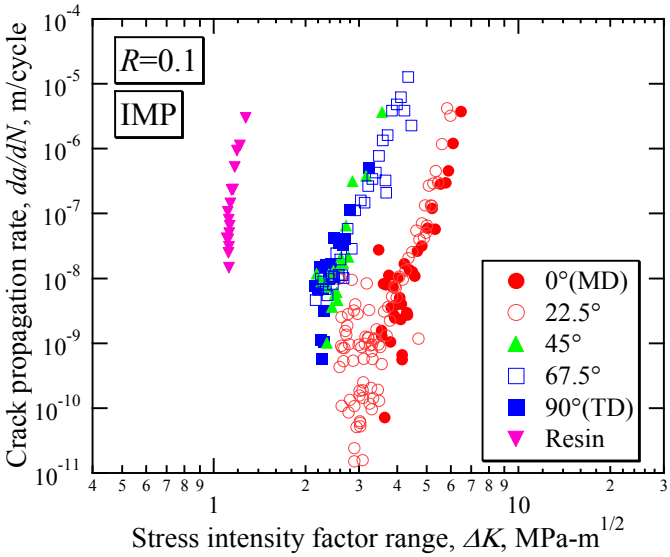

Figure 4. Relation between crack propagation rate, *da/dN,* and stress intensity range, *ΔK*, for IMP under $R = 0.1$.

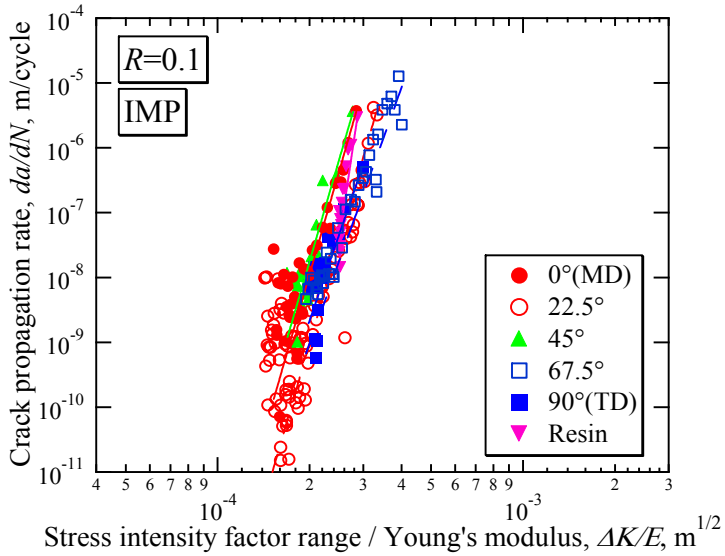

Figure 5. Relation between crack propagation rate, *da/dN,* and stress intensity range divided by Young's modulus, *ΔK/E*, for IMP under $R = 0.1$.

and TD, (3) matrix resin, where group 1 is the slowest, and group 3 is fastest. Fibers perpendicular to the crack propagation direction block crack propagation while those parallel assist crack propagation. The exponent of Paris law ranges from 9 to 30, which is higher than that for metallic materials.

Figure 5 shows the same data plotted against the ratio of *ΔK* to Young's modulus *E* which depends on the fiber angle as described in Appendix. It is interesting to see all the data merge together. The parameter, *ΔK/E,* indicates the strain intensity field near the

crack tip and often used to represent the carck propagation data for different materials [3]. The effect of the fiber orientation on the crack propagation rate mainly comes from its effect on the stiffness.

Similar results were obtained for the case of R = 0.5. Figure 6 shows the relation between da/dN and $\Delta K/E$ for MD, 45°, TD specimens under R = 0.5 together with R = 0.1. For R = 0.5, the crack propagation rate is faster and the exponent of Paris law is larger. The relations come closer in the low rate region. In Fig. 7, da/dN is plotted against the maximum stress intensity factor divided by E, K_{max}/E. In the figure, the crack propagation rate is higher for R = 0.1. Both data tend to merge at high rates, indicating unstable fracture is controlled by the K_{max} value. The crack propagation rate, da/dN, of SFRP is expressed by a power function of K_{max} and ΔK as

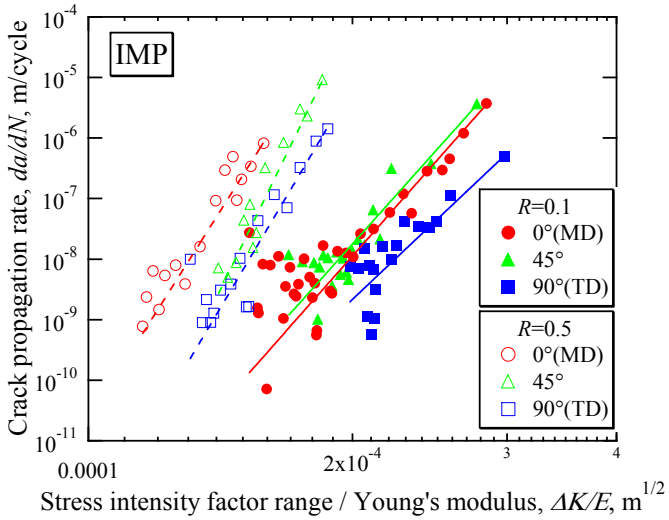

Figure 6. Relation between crack propagation rate and stress intensity range divided by Young's modulus, $\Delta K/E$, for IMP under R = 0.1 and 0.5.

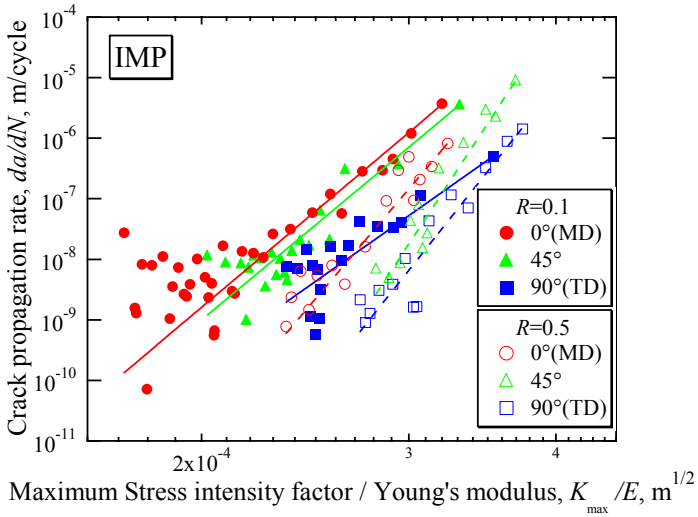

Figure 7. Relation between crack propagation rate and maximum stress intensity range divided by Young's modulus, K_{max}/E, for IMP under R = 0.1 and 0.5.

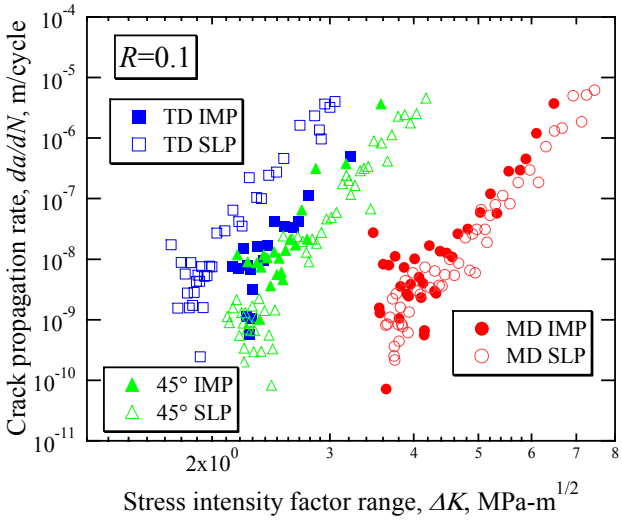

Figure 8. Relation between crack propagation rate and maximum stress intensity range for IMP and SLP under $R = 0.1$.

$$da/dN = C\left(K_{\max}{}^{\gamma} \cdot \Delta K^{1-\gamma}\right)^{m} \qquad (1)$$

where γ indicates a contribution of $K_{\max}$, and γ is close to 1 at high crack propagation rates and became smaller with decreasing rate. Similar results have been reported by Hojo *et al* [6] for long-fiber reinforced plastics.

Figure 8 shows the relation between da/dN and ΔK under $R = 0.1$ for IMP and SLP. For MD direction, the crack propagation rate of SLP is slightly lower than that of IMP, because SLP does not have the core layer of $\theta = 90^{\circ}$. For TD direction, SLP has much higher propagation rate, because it does not have the core layer of $\theta = 0^{\circ}$. The influence of the core layer on the crack propagation rate is not large in MD and 45° directions.

CONCLUSIONS

The influences of fiber orientation on the crack propagation behavior was studied with single edge-notched specimens which were cut from an injection-molded short fiber reinforced plastic plate at five fiber angles relative to the loading axis, *i.e.* θ = 0° (MD), 22.5°, 45°, 67.5°, 90° (TD). The obtained results are summarized as follows:

(1) Macroscopic crack propagation path was nearly perpendicular to the loading axis for the cases of MD and TD. For the other fiber angles, the crack path was inclined because the crack often propagated along inclined fibers.

(2) In the relation between crack propagation rate and the stress intensity factor range, ΔK, the crack propagation was slowest for MD, and increased with increasing fiber angle. When the crack propagation rate is correlated to $\Delta K/E$ (Young's modulus), all the relations merged together. The effect of the fiber orientation on the crack propagation rate mostly comes from its effect on the stiffness.

(3) The crack propagation rate was mainly controlled by ΔK at low rates and by the maximum stress intensity factor $K_{\max}$ at high rates near instability.

(4) The existence of the core layer had an influence on the fatigue crack propagation behavior of injection-molded plates. It accelerated crack propagation in MD direction, and decelerated in TD direction.

APPENDIX

Injection-molded plates used in the present study can be regarded as orthotropic and the elastic constants determined by tension test of the smooth specimens with the fiber angles, θ = 0°, 45°, and 90°, are summarized in Table 1, where suffix 1 indicates the loading axis along the fiber direction and 2 perpendicular to that. Using these values, Young's modulus for the specimen with fiber angle θ is given by [7]

$$\frac{1}{E}=\frac{\cos^4\theta}{E_1}+\frac{\sin^4\theta}{E_2}+\cos^2\theta\cdot\sin^2\theta\left(\frac{1}{G_{12}}-\frac{2\nu_{12}}{E_1}\right) \tag{2}$$

Table 2 presents the calculated value. The matrix resin was isotropic.

Table 1. Elastic constants of injection-molded plate.

E_1(GPa)	ν_{12}	E_2(GPa)	(ν_{21})	G_{12}(GPa)
22.78	0.378	10.84	(0.177)	4.86

Table 2. Young's modulus of specimens with various fiber angles.

Fiber angle	0°(MD)	22.5°	45°	67.5°	90°(TD)	Matrix
Youngs' modulus E (GPa)	22.8	18	12.9	11.1	10.8	4.45

REFERENCES

1. Voss, H. and Karger-Kocsis, J.(1988) *Int. J. Fatigue,* **Vol. 10**, pp. 3-11.
2. Wyzgoski, M. G. and Novak, G. E. (1991) *J. Mat. Sci.,* **Vol. 26**, pp. 6314-6324.
3. Akiniwa, Y., Harada, S., Yagyu, Y. and Nakano, M. (1992) *J. Soc. Mat. Sci., Japan,* **Vol. 41**, pp. 1285-1291 (in Japanese).
4. Evans, W. J., Isaac, D. H. and Saib, K. S. (1996) *Composites,* **Vol. 27A**, pp. 547-554.
5. Karger-Kocsis, J. (1989) *Applications of Fracture Mechanics to Composite Materals* (Friedlich, K. ed.) Elesevier Science Pub., pp. 189-202.
6. Hojo, M., Tanaka, K., Gustafson, C, G. and Hayashi, R. (1987) *Composite Sci. Tech.*, **Vol. 29**, pp. 273-292.
7. Carlson, L. A. and Pipes, R. B. (1987) *Experimental Characterization of Advanced Composite Materials*, Prentice Hall, Chap. 2.